ИНДЕКС 3649

АНСКИЙ ФИЗИЧЕСКИЙ ИНСТИТУТ

Preprint YERPHI-1269(55)-90

ԵՐԵՎԱՆԻ ՖԻԶԻԿԱՅԻ ԻՆՍՏԻՏՈՒՏ
ЕРЕВАНСКИЙ ФИЗИЧЕСКИЙ ИНСТИТУТ
YEREVAN PHYSICS INSTITUTE

A.M. ATOYAN

RELATIVISTIC NEUTRONS IN AGN.

II. GAMMA-RAYS OF HIGH AND VERY HIGH ENERGIES.

ЦНИИатоминформ
ЕРЕВАН-1990

Preprint YERPHI-1269(55)-90

A.M. ATOYAN

RELATIVISTIC NEUTRONS IN AGN.
II. GAMMA-RAYS OF HIGH AND VERY HIGH ENERGIES.

In the frames of the AGN model proposed in Paper I, the problem of the electromagnetic cascade in a spatially non-homogeneous field of background photons initiated due to propagation of relativistic neutrons (RNs) from the proton acceleration region $r\leq r_0\sim 10$ and their decay at large radii, $r_0<r<10^7-10^8$, is considered (the N-cascade). In contrast to the H-cascade initiated by the relativistic electrons and gamma-rays from the region of $r\leq r_0$, which is similar to the ordinary pair-photon cascades in the spatially homogeneous field of soft photons, the radiation spectra resulting from the N-cascade can be described by the power-law functions gradually steepening with increasing gamma-ray energies. The integral luminosity L_{mx} of the AGN radiation from the submillimeter to X-ray bands is the general parameter defining the N-cascade development. The features of the high-energy and very-high-energy gamma-radiation resulting from the N-cascade are investigated. It is shown that the model proposed can provide significant fluxes of very high energy ($E\geq 1$TeV) gamma-rays from the bright extragalactic sources with relatively low luminosities $L_{mx}(\leq 10^{44}-10^{45}$erg/s).

Yerevan Physics Institute

Yerevan 1990

1. Introduction

At present the most widespread idea concerning the main powerhouse for electromagnetic radiation of active galactic nuclei (including quasars, hereafter AGN) is that gravitational potential energy of matter accreting onto a supermassive black hole (BH) is responsible for their extremely high luminosities (e.g., see review papers [1,2]). One of the arising problems then is to provide high efficiencies of the rest-mass to radiation energy conversion $\eta=L/\dot{M}c^2\sim 0.1$, (L and $\dot{M}$ being the luminosity and the accretion rate, respectively), otherwise the high luminosities of AGN comparable with their Eddington ones (e.g., for Seyfert galaxies $L/L_{Edd}\leq 0.5$, see [3]) would require dimensionless accretion rates $\dot{m}=\dot{M}c^2/L_{Edd}\gg 10$. The characteristic timescale for a significant increase of the mass of AGN (or supposed BH), $\Delta t_M=M/\dot{M}=(4.5/\dot{m})\cdot 10^8$yr, being taken into account, these high accretion rates seem to be inconsistent with a presumable "lifetime" of AGN, $t_{AGN}\geq 10^8$yr [4].

Since the maximal energy per proton in accretion plasma at the dimensionless distance $r\equiv R/R_g$ from BH cannot exceed $m_pc^2/2r$, (R_g being the gravitational radius), then, obviously, the magnitudes of $\eta\sim 0.1$ may be achieved only in the case when in the range $r\leq r_0\sim 10$ a significant fraction of the kinetic

possibilities can lead, in particular, to realization of the accretion plasma turbulent reactor (APTR) model considered in [2]. In this paper we suppose that the first cooling mechanism dominates. In this case the relativistic electrons (both e^+ and e^-) and gamma-rays, resulting from the decay of secondary particles (predominantly of pions) in pp collisions, initiate the electromagnetic cascade of electrons and gamma-quanta in the background field of low-frequency (from submillimeter to X-ray bands) photons. It should be stressed at once, that the relatively small, dense BL clouds occupy a negligible fraction of the volume of AGN. Therefore here they can be considered only as numerous sites for the RP energy sink and of production of initial gamma-rays and electrons, whereas the cascade is developed generally in the intercloud space.

The gamma-ray spectra resulting from the electromagnetic cascade in spatially homogeneous field of background soft photons in compact sources have been considered earlier in [3-7] (hereafter, H-cascade). In the model under consideration the electromagnetic cascade of this type (in the homogeneous field of soft photons at $r\leq r_{mx}$, see paper I) is in fact initiated by the gamma-rays and electrons produced in the RP acceleration range $r\leq r_0$. The main goal of this paper, however, is to investigate the electromagnetic cascade that is due to radial propagation of RNs outward the main power-house of AGN. Two general features of this cascade are, that (a) it is developed in spatially non-homogeneous field of the low-frequency photons with the number density decreasing as r^{-2} at $r>r_{mx}$, and (b) the characteristic energy of initial cascade-initiating particles, resulting from the neutron decay and further nuclear pp interactions, linearly increases with

increasing r (see Paper I). The combination of these two factors brings to the spectra of high-energy gamma-rays, resulting from that cascade (hereafter, N-cascade), quite different from the spectra resulting from the H-cascades, considered previously. In the model under consideration the H-cascade in the region of $r_0<r<r_{max}$ is responsible for the resulting spectra of gamma-rays with moderate energies, $E\leq 100$MeV. Below we consider the possibility for gamma-rays of much higher energies, $100\text{MeV}\leq E\leq 100\text{TeV}$, to escape from AGN due to the N-cascade developed at distances $r_0\leq r\leq r_a\sim 10^7-10^8$.

2. Initial Production Functions

To find the production functions of initial electrons and gamma-rays in the range $r_0\leq r\leq r_a$, the equilibrium local spectra of the secondary protons resulting predominantly from the decay of the RNs with Lorentz-factors $\Gamma_n\leq\Gamma_{esc}\sim 10^7-10^8$ (see paper I) should be first obtained. At large distances from the RP acceleration region, $r\gg 10$, the secondary RP production is owing mainly to the decay of RNs with characteristic Lorentz-factors

$$\Gamma_d = a_d r \qquad (II.1)$$

with $a_d=1.1M_8$. Below at all radii $r>r_0$ only this process is taken into account, the contribution from $n\gamma$ collisions in the region $r_0<r<r_{mx}\sim 10^2-10^3$ being neglected. Notice that this approximation is absolutely accurate for the power-law spectra of the RNs with the maximal Lorentz-factors Γ_{max} not exceeding $\Gamma_{esc}\sim 10^7-10^8$ (see Eq.(I.21)). From Eqs.(I.31-I.37) the relevant secondary RP production spectrum is obtained:

$$q_p(r,x)=Bx^{-(\alpha+1)}\exp\left(-\frac{a_d m_p r}{m_e x}\right)r^{-2} \qquad (II.2)$$

where $x\equiv E_p/m_e c^2$ is the dimensionless energy of the protons, and

$$B = \frac{\eta_n \dot{m} L_{Edd}(\alpha-2)}{4\pi m_p c^3 R_g^2 \tau_0 (1-\Gamma_0^{2-\alpha})}\left(\frac{m_p}{m_e}\right)^{\alpha+1} . \qquad (II.3)$$

Here $\Gamma_0=\min\{\Gamma_{max},\Gamma_{esc}\}$, $\tau_0\simeq 900s$ is the neutron lifetime, and $\eta_n\sim 0.03$ is the efficiency of the rest-mass-to-RN-energy conversion in the RP acceleration region $r\leq r_0$.

Suppose now that $\nu_{eff}\equiv\nu_{eff}(r)$ is the effective frequency of the pp collisions of these protons at a given r. Then the energy loss rate of the RPs can be written as

$$\dot{x} = -\nu_{eff} K_p x . \qquad (II.4)$$

Here $K_p(\sim 0.5)$ is the inelasticity coefficient at pp collisions. The equilibrium spectra of the local RP distribution functions can be found from the standard kinetic equation in the continuous energy loss approximation, resulting in

$$N_p(r,x) = \frac{1}{-\dot{x}}\int_x^\infty q_p(r,x_1)dx_1 . \qquad (II.5)$$

With account of Eq.(II.2) one may see that $N_p(r,x)\propto 1/x$ at $x\ll x_d\equiv(m_p/m_e)\Gamma_d$, and $N_p(r,x)\propto x^{-(\alpha+1)}$ for $x\gg x_d$. Note that the main part of the RP energy is in the range of $x\sim x_d$, where the transition from the hard to the soft power-law behaviour of this spectrum takes place.

Consider now the local (at given r) production spectra of the relativistic electrons, the gamma-rays, and the neutrinos, resulting from the decays of the secondary particles (mainly of pions) produced in the nuclear pp interactions:

$$p + p \rightarrow N + \sum_{i=1}^{n_s} \pi_i , \qquad (II.6)$$

$$\pi^0 \rightarrow 2\gamma , \qquad (II.7)$$

$$\pi^\pm \rightarrow \mu^\pm + \nu_\mu \rightarrow e^\pm + \nu_e + 2\nu_\mu . \qquad (II.8)$$

Here N is for the leading nucleon (the proton or the neutron), and n_s is the multiplicity of the secondary pions. At these collisions the mean energy of the leading nucleon amounts the fraction $(1-K_p)=0.57\pm 0.01$ of the incident proton energy E_p, and the remaining fraction $K_p=0.43\mp 0.01$ of E_p is carried away mainly by a few energetic pions (see, e.g., [8]). Since the mean energy of each from these pions is $\langle E_\pi\rangle\simeq 0.15E_p$, we note that the inelasticity K_p corresponds on the average to production of three energetic pions per each collision. Taking further into account, that at multiplicities n_s sufficiently high (practically, at energies $E_p>100GeV$) the probability to observe the energetic pions are almost the same for π^0, π^+ and π^-, the sum $\sum_{i=1}^{n_s}\pi_i$ in the right hand side of Eq.(II.6) may be in effect substituted by $(\pi^0+\pi^++\pi^-)$ with the energy of each pion $E_\pi=0.15E_p$ (corresponding to the inelasticity $K_p=0.45$). This approach corresponds to δ-functional approximation to the differential cross-section for production of energetic pions of different signs s=0,+,- : $d\sigma_s(E_\pi)/dE_\pi=\sigma_{pp}\delta(E_\pi-0.15E_p)$, with $\sigma_{pp}\simeq 4\cdot 10^{-26}cm^2$. This approximation enables to estimate the relevant production functions of the pions and of their decay products with energies $E\geq 100MeV$. For energies $E\leq 100MeV$ the δ-functional approximation cannot be applied. At these energies the resulting electrons, gamma-rays, and neutrinos have flat

spectra.

Since at the decay of the π^0-meson the mean energy per gamma-quantum produced is $\langle E_\gamma \rangle = 0.5E_\pi = 0.075E_0$, the gamma-ray production function at given r can be estimated as:

$$q_\gamma^{(0)}(r,\varepsilon) = 2\nu_{eff} \frac{N_p(r,\varepsilon/0.075)}{0.075} . \qquad \text{(II.9)}$$

To find the characteristic energies of the secondary particles in the decays of charged pions, mind that the muon neutrino produced at the pion decay, $\pi^\pm \to \mu^\pm + \nu_\mu$, on the average carries the $[1-(m_\mu/m_\pi)^2]/2 \simeq 0.21$ fraction of the initial pion energy. Taking further into account, that the mean energy of each secondary particle resulting from the muon decay is approximately equal to the 1/3 of the muon energy (since in the muon rest frame the electron is relativistic, $E_e = p_e c$), we obtain that the electron carries on the average $\simeq 26\%$ of the initial pion energy. For $E_\pi = 0.15E_p$ this corresponds to $\langle E_e \rangle \simeq 0.039E_p$. The neutrinos carry the remaining $\simeq 74\%$ of the pion energy, therefore the mean energy per neutrino $\langle E_\nu \rangle \simeq 0.037E_p$. (The mean energy of the first muon neutrino is slightly smaller, and the mean energies of the second ν_μ and of the ν_e are slightly greater, than this value. It is obvious, however, that for qualitative considerations this difference can be neglected). So, in the δ-functional approximation used, the production spectra of the electrons (both e^+ and e^-) and the neutrinos can be written as:

$$q_e^{(0)}(r,\gamma) = \frac{2\nu_{eff}}{0.039} N_p(r,\gamma/0.039) , \qquad \text{(II.10)}$$

$$q_\nu(r,\varepsilon) = \frac{2\nu_{eff}}{0.037} N_p(r,\varepsilon/0.037) . \qquad \text{(II.11)}$$

Here γ is the electron Lorentz-factor (this variable should not

be confused with the similar notation γ for gamma-rays, e.g., at $\gamma\gamma$ collisions). It is worth noting, that since the RP distribution function $N_p \propto 1/\nu_{eff}$, then the production functions in Eqs.(II.9-II.11) depend only on the local production rate of the RPs, $q_p(r,x)$, and do not depend on the local pp collision frequency ν_{eff}.

Taking into account that the secondary gamma-rays, electrons and neutrinos carry away $K_p = 0.45$ fraction of the incident proton energy per collision, the resulting distribution of the local power $\dot{E}_p \equiv \dot{E}_p(r)$ released initially in the RPs between these secondaries can be readily found, $\dot{E}_s/\dot{E}_p = \langle E_s \rangle / E_p K_p$. Then,

$$\dot{E}_\gamma/\dot{E}_p = 0.33 , \qquad \text{(II.12)}$$

$$\dot{E}_e/\dot{E}_p = 0.18 , \qquad \text{(II.13)}$$

$$\dot{E}_\nu/\dot{E}_p = 0.49 . \qquad \text{(II.14)}$$

So, in the model under consideration half of the total power $\dot{W}_n$, transported by the RNs from the RP acceleration region $r \le r_0$, goes at large r to the neutrino production, whereas the second half of $\dot{W}_n$ is transformed to the relativistic electrons and gamma-rays initiating the N-cascade in the region $r_0 < r < 10^7 - 10^8$. The differential flux of those neutrinos is obtained by integrating Eq.(II.11) over the AGN volume. In the range of dimensionless energies $0.037 m_p/m_e < \varepsilon < 0.037 \Gamma_0 m_p/m_e$ this results in the neutrino flux

$$\dot{N}_\nu^{(n)}(\varepsilon) = 0.49 \frac{\eta_n \dot{m} L_{Edd} (\alpha-2)}{m_e c^2 (1-\Gamma_0^{2-\alpha})} \left[0.037 \frac{m_p}{m_e}\right]^{\alpha-2} \varepsilon^{-\alpha} , \qquad \text{(II.15)}$$

repeating the power-law spectrum of the RPs in the acceleration range $r \le r_0$. Note, that the total flux of neutrinos escaping AGN is determined by both the neutrinos produced at $r > r_0$, and the ones created directly in the RP acceleration region $r \le r_0$. Taking into account that in this region the powers $\dot{W}_n \simeq \dot{W}_\nu \simeq \dot{W}_p/3$ (see paper I), and that the flux given by Eq.(II.15) corresponds to the half of the RN power $\dot{W}_n$, the total neutrino flux can be estimated as $\dot{N}_\nu^{(tot)} \simeq 3\dot{N}_\nu^{(n)}$. So, about half of the RP acceleration power $\dot{W}_p = \eta_p \dot{M} c^2$ is carried out from the acceleration range $r \le r_0$ by the neutrinos. About the 1/3 of $\dot{W}_p$ is transformed into relativistic electrons and gamma-rays in the region $r < r_0$, which then initiate the H-cascade in the region $r_0 \le r \le r_{mx}$. The remaining $\sim$1/6 of $\dot{W}_p$, or $\sim \dot{W}_n/2$, goes to production of ultrarelativistic electrons and gamma-rays, initiating the N-cascade at distances $r_0 < r < r_a \sim 10^7 - 10^8$.

3. The Main Processes and Parameters of the Cascade

The following processes can be important for development of an electromagnetic cascade in the background field $n_0(r,\varepsilon_0)$ of soft photons:

a) the photoproduction of e^+-e^- pairs at photon-photon collisions;

b) the inverse Compton scattering (ICS) of the relativistic electrons off the soft photons;

c) the synchrotron emission of the electrons in the ambient magnetic field B(r);

d) the bremsstrahlung and the ionization energy losses of the electrons in the thermal accretion plasma;

e) the e^+-e^- annihilation of the relativistic positrons on

the ambient thermal negatrons.

In compliance with the paper I, the background soft photons are described by the spectral number density

$$n_0(r,\varepsilon_0) = \frac{\dot{W}_0}{m_e c^2} \varphi_r(r) \varphi_0(\varepsilon_0)/\varepsilon_0 \ , \qquad (II.16)$$

where $\varphi_r \equiv \varphi_r(r)$ and $\dot{W}_0$ are given by Eqs.(I.3) and (I.4), respectively. Since the spectral luminosity of AGN in the range from submillimeter wavelengths up to X-rays can be generally described by the power-law index $\alpha_{mx} \ge 1$, whereas in the radio-to-submillimeter range the spectra are flat or inverted, for the numerical calculations below we suggest the background photon spectra of the form

$$\varphi_0(\varepsilon_0) = A \frac{\varepsilon_0^{\alpha_{rm}}}{(\varepsilon_0+\varepsilon_c)^{\alpha_{mx}+\alpha_{rm}}} \qquad (II.17)$$

for the "soft" photon dimensionless energy ε_0 up to $\varepsilon_0 \sim 1$. Here $\varepsilon_c (\sim 10^{-7})$ is the characteristic energy, corresponding to the low-frequency cutoff (or flattening) of the spectrum in submillimeter-IR range (for $\varepsilon_c = 10^{-7}$ the cutoff frequency $\nu_c = m_e c^2 \varepsilon_c / h \simeq 10^{13}$ Hz). The coefficient A corresponds to the normalization $\int \varphi_0 d\varepsilon_0 = 1$. For analytical estimations further on we use the typical power-law index $\alpha_{mx} = 1$. In the numerical calculations the spectra with different $\alpha_{mx} \ge 1$ and $\alpha_{rm} \ge 0$ in Eq.(II.17) are considered.

It should be noted here that Eq.(II.16) represents the spectral number density of the background photons, integrated over their propagation directions. Therefore, to utilize this number density in further calculations, we should assume, strictly speaking, that the local distributions of the

background radiation are isotropical. Obviously, this is valid in the region $r \le r_{mx}$ responsible for this radiation, whereas at $r \gg r_{mx}$ the photons propagates radially outwards. Nevertheless, at these large radii also the Eq.(II.16) can be used for calculation of the ICS gamma-ray production functions averaged over directions of incident relativistic electrons. This is possible as the electrons quickly become isotropical in ambient tangled magnetic fields. Some anisotropy of those production functions, as well as the pronounced radial anisotropy of the background radiation field at large r, should not have an essential impact on the N-cascade, since the gamma-ray absorption coefficient $\varkappa_{\gamma\gamma}(r,\varepsilon,\theta)$ (per unit dimensionless pathlength dl) at photon-photon collisions essentially differs from the mean, $\bar{\varkappa}_{\gamma\gamma}(r,\varepsilon)$ (averaged over the collision angle θ between the gamma-ray wave vector $\vec{k}$ and the radius-vector $\vec{r}$), only for a small fraction of the cascade gamma-rays, namely, for the ones propagating inside a narrow cone with $(1-\cos\theta) \ll 1$. For all other directions of $\vec{k}$ the value of $\varkappa_{\gamma\gamma}(r,\varepsilon,\theta)$ is close to the mean, $\bar{\varkappa}_{\gamma\gamma} \equiv \bar{\varkappa}_{\gamma\gamma}(r,\varepsilon)$. Some difference between them should not have a significant effect on the gamma-ray spectra resulting from the N-cascade, since in those cases when the gamma-rays are produced in the region r opaque to absorption, $\bar{\varkappa}_{\gamma\gamma} \cdot r > 1$, they are absorbed in the same space region they were produced, whereas in case of their production in the optically transparent region $\bar{\varkappa}_{\gamma\gamma} r < 1$, the gamma quanta leave the spherical source, both irrespective of the anisotropy of the local absorption coefficient. The accretion plasma density in the region up to the accretion radius, $r \le r_a$, is given by Eq.(I.1). The characteristic magnitude of tangled magnetic field, B(r), in the accretion plasma is determined from the assumption that

its energy density amounts to some fraction $\delta_B \le 1$ of the thermal electron energy density in the plasma, which yields [2]:

$$B(r) \simeq 1.4 \cdot 10^4 \, \delta_B^{1/2} \, \dot{m} \, M_8^{-1/2} \begin{cases} r^{-5/4}, & r \ge r_* \\ r_*^{-1/2} \, r^{-3/4}, & r < r_* \end{cases} \quad G \quad . \qquad (II.18)$$

Here $r_* \sim 10^3$ is the critical radius below which the plasma becomes a two-temperature one, $T_p > T_e$, with $T_e \simeq \text{const} \le 10^9$ K.

a) Photoproduction of e^+-e^- pairs.

The production spectrum $q_e(r,\gamma)$ of the electrons (both e^+ and e^-), in unit volume per unit time due to absorption of gamma-rays in the field $n_0(r,\varepsilon_0)$ of soft photons, is determined using the relevant cross-section $\sigma_{\gamma\gamma}(\gamma,\varepsilon_0,\varepsilon)$ calculated in Ref.[9]. The spectrum can be presented as

$$q_e(r,\gamma) = \varphi_r \int S_{\gamma\gamma}(\gamma,\varepsilon) \, n_\gamma(r,\varepsilon) \, d\varepsilon \, , \qquad (II.19)$$

with

$$S_{\gamma\gamma}(\gamma,\varepsilon) = \frac{2cW_0}{m_e c^2} \int \sigma_{\gamma\gamma}(\gamma,\varepsilon_0,\varepsilon) \, \frac{\varphi_0(\varepsilon_0)}{\varepsilon_0} \, d\varepsilon_0 \, . \qquad (II.20)$$

Here $n_\gamma(r,\varepsilon)$ is the spectral number density of gamma-rays with the dimensionless energy $\varepsilon = E/m_e c^2$. The factor 2 in Eq.(II.20) corresponds to creation of two electrons per collision. Then the frequency of photon-photon collisions is:

$$\nu_{\gamma\gamma}(r,\varepsilon) = \varphi_r \int_1^\varepsilon S_{\gamma\gamma}(\gamma,\varepsilon) \, d\gamma/2 \, . \qquad (II.21)$$

For analytical estimations the relevant expression of Herterich [10], resulting in

$$\nu_{\gamma\gamma}(r,\varepsilon) \simeq \frac{5}{4} \frac{\sigma_0 W_0}{m_e c} \, \varphi_r \, \varphi_0(4/\varepsilon), \qquad (II.22)$$

where $\sigma_0=1.7\cdot10^{-25}cm^2$, may be used. For the typical spectrum $\varphi_0\propto\varepsilon_0^{-1}$ at $\varepsilon_0>\varepsilon_c$, the optical thickness of the source in the region $\sim r$ with respect to absorption of a gamma-ray with energy $\varepsilon<1/\varepsilon_*$ is estimated as

$$\tau_{\gamma\gamma}(e,\varepsilon) \simeq 0.4\left(L_{mx}/0.1L_{Edd}\right)r^{-1}\,\varepsilon\ , \qquad (II.23)$$

Then there can be found the maximal energy of gamma-rays that can escape AGN from the radii $\sim r$ ($>r_{mx}$):

$$\varepsilon \le \varepsilon_{esc} = 2.5\left(L_{mx}/0.1L_{Edd}\right)^{-1}r\ . \qquad (II.24)$$

One easily concludes from this equation, that the high-energy (HE) gamma-rays, $E_\gamma>1GeV$ (or dimensionless $\varepsilon>2000$), can escape AGN only if they are emitted at large distances from the BH, $r\ge10^3$. Very high energy (VHE) gamma-rays, $E\ge1TeV$, should be produced at much larger radii, $r\ge10^6$, to be able to leave the source.

Let us now estimate the characteristic energy $\varepsilon_{in}(r)$ of the initial gamma-rays at a given r, resulting from inelastic pp interactions and further decay of the secondary π-mesons. Taking into account that the characteristic energy of these gamma-rays is related with the energy of parent RPs as $E_\gamma\sim0.1E_p$, and using the Eq.(II.1), we obtain:

$$\varepsilon_{in}(r) \simeq 200\ M_8\ r\ . \qquad (II.25)$$

Then it follows from Eq.(II.24) and Eq.(II.25), that at $r>r_{mx}$ the ratio $\varepsilon_{in}/\varepsilon_{esc}$ depends only on the integral luminosity L_{mx} in the soft photons, being independent of r. For typical AGN masses $0.1\le M_8\le10$ and luminosities $L_{mx}\sim0.1L_{Edd}$ under consideration (corresponding to $10^{44}\le L_{mx}\le10^{46}$ erg/s) this ratio is within $10\le\varepsilon_{in}/\varepsilon_{esc}\le10^3$. In this case the electromagnetic N-cascade in AGN should be developed.

b) ICS of electrons.

The characteristic Compton cooling time $t_c(r,\gamma)$ of the relativistic electrons being considered, note that the main contribution to the energy loss rate $\dot\gamma\equiv(\partial\gamma/\partial t)$ is due to electron scattering off the soft photons for which the parameter $b\equiv4\gamma\varepsilon_0<1$ (i.e., the ICS scattering in Thomson limit), whereas the contribution to $\dot\gamma$ due to electron scattering off the photons with $\varepsilon_0>1/4\gamma$ corresponding to the Klein-Nishina limit is negligible. (As it is shown by Zdziarskii [11], even for the extremely hard spectra of the soft photons with $\alpha_{mx}\sim0$, the main contribution to the energy losses of electrons is due to the photons in the energy range $\varepsilon_0<1/4\gamma$). Therefore, to estimate the Compton cooling time $t_c(r,\gamma)=\gamma/|\dot\gamma|$, we can use the known equation $m_ec^2\dot\gamma=-(4/3)\sigma_T c\gamma^2W_\gamma$ [12], where the energy density W_γ at given γ relates to the soft photons energy density in the range $\varepsilon_0\le1/4\gamma$. Then using Eqs.(II.16) and (II.17), for electrons in the energy range $\gamma\ll\gamma_*\equiv\varepsilon_c^{-1}$ we find:

$$t_c(r,\gamma) \simeq 8.3\ M_8\ \left(L_{mx}/0.1L_{Edd}\right)^{-1}\gamma^{-1}\varphi_r^{-1}\ ,\ (s)\ . \qquad (II.26)$$

Comparing Eq.(II.26) with the characteristic accretion time of plasma,

$$t_a(r) \simeq 2\cdot10^3\ M_8\ r^{3/2}\ ,\ (s), \qquad (II.27)$$

we conclude, that at all radii $r\le r_a$ and at least for $\gamma>100$ the spectra $n_e(r,\gamma)$ of relativistic electrons are defined by the local production and cooling processes.

The spectrum of gamma-rays produced at ICS of relativistic electrons can be written in the form:

$$q_\gamma(r,\varepsilon) = \varphi_r\int S_c(\varepsilon,\gamma)\ n_e(r,\gamma)\ d\gamma\ . \qquad (II.28)$$

Here $S_c(\varepsilon,\gamma)$ is the gamma-ray spectrum produced at the ICS of

an electron with a given γ:

$$S_c(\varepsilon,\gamma) = \frac{cW_0}{m_e c^2} \int \sigma_c(\varepsilon_0,\varepsilon,\gamma)\, \varphi_0(\varepsilon_0)\, \frac{d\varepsilon_0}{\varepsilon_0}\,, \qquad \text{(II.29)}$$

where $\sigma_c(\varepsilon_0,\varepsilon,\gamma)$ is the relevant differential cross section calculated in Ref.[13]. Since for the electromagnetic cascade the efficiency of emission of gamma-rays with energies ε comparable with the initial electron energy γ is very important, it is of interest to consider the characteristic efficiency of the Compton process with respect to emission of energetic gamma-rays:

$$\eta_c(x) = \frac{\int_{x\gamma}^{\gamma} \varepsilon\, S_c(\varepsilon,\gamma)\, d\gamma}{\int_{1}^{\gamma} \varepsilon\, S_c(\varepsilon,\gamma)\, d\gamma} \qquad \text{(II.30)}$$

with $x \equiv \varepsilon/\gamma \le 1$. In Fig.1 the ICS efficiencies $\eta_c(x)$ for different α_{mx} and $\varepsilon_c\gamma$ are presented.

c) Synchrotron Radiation

Since the characteristic frequency of synchrotron photons is $\nu_s \simeq 0.3\nu_B\gamma^2$ with $\nu_B \equiv eB/2\pi m_e c$ (see [14]), the dimensionless energy of these photons, $\varepsilon_s = h\nu_s/m_e c^2$, is reduced to

$$\varepsilon_s(r) = 3\cdot 10^{-10} \delta_B^{1/2}\, \dot{m}^{1/2}\, M_8^{-1/2}\, \gamma^2 \begin{cases} r^{-5/4}, & r \ge r_* \\ r_*^{-1/2}\, r^{-3/4}, & r < r_* \end{cases} . \qquad \text{(II.31)}$$

Then, using Eq.(II.25) for typical energies of initial gamma-rays and electrons at a given r we calculate that the maximum energy of synchrotron photons is reached at large radii, $r \le 10^8$, and corresponds to X-rays. Therefore, the account

of synchrotron radiation should lead to significant decrease of HE and VHE gamma-ray flux escaping AGN if the characteristic synchrotron cooling time $t_s(r,\gamma)$ of the cascade electrons would be comparable with or less than their Compton cooling time $t_c(r,\gamma)$. Using Eq.(II.18) for the magnetic field B, we find:

$$t_s(r,\gamma) \simeq 3.9\, \delta_B^{-1}\, \dot{m}^{-1}\, M_8\, \gamma^{-1} \begin{cases} r^{5/2}, & r \ge r_* \\ r_* r^{3/2}, & r < r_* \end{cases} , \text{(s)}. \qquad \text{(II.32)}$$

From comparison of Eqs.(II.32) and (II.26) we conclude that the ratio t_c/t_s decreases with increasing r. For the N-cascade in the region of $r \ge 10^3$ responsible for formation of the spectra of HE gamma-rays escaping AGN, the Eqs.(II.26) and (II.32) bring to the ratio $t_c/t_s \le 0.1$. Note, however, that Eq.(II.26) for the Compton cooling time is valid for the electron energies $\gamma \ll \gamma_* \equiv 1/\varepsilon_c$. Accurate numerical calculations show that $t_c(r,\gamma)$ may be significantly higher than the one corresponding to Eq.(II.26) (see Fig.2). It means that the efficiency of N-cascade for the VHE gamma-rays may be affected by the magnetic field in a greater extent, than in the HE range, $\varepsilon \ge 10^3$ ($E \ge 1$GeV).

c) Ionization and Bremsstrahlung Energy Losses of Electrons

The electron energy loss rates in these processes are defined by the expressions:

$$-\dot{\gamma}_{ion} = 2\pi r_e^2\, n_T c A_{ion}\,, \qquad \text{(II.33)}$$

$$-\dot{\gamma}_{br} = 2\pi r_e^2\, n_T c \gamma A_{br}\,, \qquad \text{(II.34)}$$

where $r_e \simeq 2.8\cdot 10^{-13}$cm is the classical radius of electron. For fully ionized plasma $A_{ion} \sim 70$ and $A_{br} \sim 0.1$ (see, e.g. [12]).

Using the Eq.(I.1) for the accretion plasma density n_T, the ionization cooling time can be found:

$$t_{ion} \simeq 20\ \dot{m}^{-1}\ M_8\ r^{3/2}\gamma\ ,\ (S). \qquad (II.35)$$

It follows from comparison of Eqs.(II.26) and (II.35) that in the whole accretion region $r \le r_a$ ($\le 10^8$) and at least for electrons with $\gamma \ge 10^2$ the ICS energy losses significantly exceed the ionization ones.

From Eqs.(II.33) and (II.34) we can see that for moderately relativistic electrons, $\gamma \le 100$, the bremsstrahlung energy losses are significantly less than ionization losses ($t_{br} \gg t_{ion}$), whereas for more energetic electrons the Compton cooling dominates throughout the whole volume of AGN. In Fig.2 the cooling times, t_{ion}, t_{br}, and t_c, related to synchrotron cooling time t_s, are shown. Obviously, at all energies the bremsstrahlung losses can be neglected.

d) e^+e^- Pair Annihilation

The relativistic positrons produced at photon-photon collisions may annihilate on the ambient thermal electrons of the accretion plasma. Using the annihilation cross section of relativistic positrons with $\gamma \gg 1$, $\sigma_{an} \simeq \pi r_e^2 \ln\gamma/\gamma$ (e.g., see [15]), the annihilation time $t_{an}=(\sigma_{an} c n_T)^{-1}$ is obtained:

$$t_{an} = 2.7\cdot 10^3\ \dot{m}^{-1}\ M_8\ r^{3/2}\ \gamma\ \ln^{-1}\gamma\ ,\ (S). \qquad (II.36)$$

Comparing this with Eq.(II.26) we see that already at $\gamma \ge 100$ the Compton cooling rate exceeds the positron annihilation rate at least by two orders of magnitude. It means that annihilation of relativistic positrons is not important for the HE pair-photon

cascade. Moreover, this process is not significant at lower energies ($\gamma < 100$) as well, since even in the extreme case when both the Compton and the synchrotron energy losses are completely neglected, no more than ~20% of the positrons may annihilate prior to be thermalized in the accretion plasma due to ionization losses only [16].

4. Kinetic Equation for Relativistic Electrons

As is shown above, the spectral number density $n_e(r,\gamma)$ of electrons (both e^+ and e^-) is defined by the local (at a given r) processes of their production and cooling. Then, at all r the equation describing $n_e(r,\gamma)$ is similar to the familiar stationary kinetic equation in a spatially homogeneous space (see, e.g., BG [13] or Zdziarskii [11]):

$$q_e(r,\gamma) - n_e(r,\gamma)\int c_r(\gamma,\gamma_1)d\gamma_1 + \int c_r(\gamma_1,\gamma) n_e(r,\gamma_1) d\gamma_1 = 0, \qquad (II.37)$$

where $q_e(r,\gamma)$ is the electron production spectrum (per unit time and in unit volume), and $c_r(\gamma,\gamma_1)$ is the probability of electron transition (in unit time) from a state with energy γ to a state with energy γ_1. For the Compton process $c_r^{(c)}(\gamma,\gamma-\varepsilon)=\varphi_r S_c(\varepsilon,\gamma)$, where $S_c(\varepsilon,\gamma)$ is defined by the Eq.(II.29). In the general case each process contributes additively to the resulting kernel of Eq.(II.37), i.e. $c_r=\sum_i c_r^{(i)}$.

The electron production function $q_e(r,\gamma)$ includes both the initial production function $q_e^{(0)}$ of Eq.(II.10) and the e^+e^- pair production given by Eqs.(II.19) and (II.20). In principle, the annihilation term for relativistic positrons should be also included in $q_e(r,\gamma)$ with the negative sign. However, as it has

been shown above, this process can be neglected.

In the continuous energy loss approximation ($\Delta\gamma/\gamma \ll 1$) the distribution of the relativistic electrons is written similar to Eq.(II.5) for RPs:

$$n_e(r,\gamma) = \frac{1}{-\dot{\gamma}} \int_{\gamma}^{\infty} q_e(r,\gamma_1) d\gamma_1 , \qquad (II.38)$$

where $\dot{\gamma}$ is the dimensionless energy loss rate of electrons. In the catastrophic energy loss limit, when the electron may lose a significant fraction of its energy in a single collision ($\Delta\gamma/\gamma \to 1$), the analytical solution of Eq.(II.37) in the general case is not obtained. In a particular case, when electrons lose their energy at ICS in the field of soft photons having hard spectra $n_0(\varepsilon_0) \propto \varepsilon^{-\alpha}$ with $0<\alpha<2$, the analytical solution of Eq.(II.37) has been suggested by Zdziarskii [11].

In this section we suggest a solution of Eq.(II.37) in δ-functional approximation to the kernel $C_r(\gamma,\gamma_1)$, which in principle allows us to consider arbitrary production functions q_e, and to take into account, along with Compton losses, other kinds of energy losses (in particular, synchrotron and ionization losses) as well.

Let the mean energy lost by the electron per collision be equal to $\Delta \equiv \Delta(r,\gamma)$, and the collision frequency $\nu_e \equiv \nu_e(r,\gamma)$. Note that

$$\nu_e(r,\gamma) = \int_1^{\gamma} d\gamma_1 \; C_r(\gamma,\gamma_1) , \qquad (II.39)$$

$$\Delta(r,\gamma) = \frac{1}{\nu_e(r,\gamma)} \int_1^{\gamma} (\gamma-\gamma_1) \; C_r(\gamma,\gamma_1) \; d\gamma_1 . \qquad (II.40)$$

The δ-functional approximation for the kernel $C \equiv C_r$ of the integral Eq.(II.37) (hereafter in this section we omit r for convenience) satisfying Eqs.(II.39) and (II.40) is written as:

$$C(\gamma,\gamma_1) = \nu_e(\gamma) \; \delta(\gamma_1 - \gamma + \Delta(\gamma)) . \qquad (II.41)$$

Then Eq.(II.37) is reduced to

$$q_e(\gamma) - \nu_e(\gamma) n_e(\gamma) + \left. \frac{\nu_e(\gamma_1) n_e(\gamma_1)}{1 - \frac{\partial \Delta(\gamma_1)}{\partial \gamma_1}} \right|_{\gamma_1 = \gamma + \bar{\Delta}(\gamma)} \qquad (II.42)$$

Here $\bar{\Delta}(\gamma)$ is the function "inverse" to $\Delta(\gamma)$ defined by the condition:

$$\text{if} \quad \gamma' = \gamma - \Delta(\gamma) , \qquad (II.43)$$

$$\text{then} \quad \gamma = \gamma' + \bar{\Delta}(\gamma') \qquad (II.44)$$

Denoting $F_\gamma \equiv n_e \nu_e$, the Eq.(II.42) is rewritten as:

$$F(\gamma) = q_e(\gamma) + D(\gamma_1) \; F(\gamma_1) , \qquad (II.45)$$

where $D(\gamma) \equiv 1/(1-\partial\Delta/\partial\gamma)$, and $\gamma_1 = \gamma + \bar{\Delta}(\gamma)$. To solve this equation, we define the following sequence $\{\gamma_i\}_\gamma$ of discrete γ_i for a given γ:

$$\gamma_0 = \gamma ;$$

$$\gamma_i = \gamma_{i-1} + \bar{\Delta}(\gamma_{i-1}) , \text{ at } \quad i \geq 1. \qquad (II.46)$$

Then the Eq.(II.45) is reduced to the sequence of chained equations

$$F(\gamma_i) = q_e(\gamma_i) + D(\gamma_{i+1}) \; F(\gamma_{i+1}) , \qquad (II.47)$$

where $i \geq 0$. The solution of this equation is found by substitutions resulting in the expression for $n_e = F_e/\nu_e$:

$$n_e(\gamma) = \nu_e^{-1}(\gamma) \left\{ q_e(\gamma) + \sum_{i=1}^{\infty} \left[q_e(\gamma_i) \prod_{j=1}^{i} D(\gamma_j) \right] \right\} . \qquad (II.48)$$

($\prod$ is the multiplication symbol). Taking into account that for realistic production spectra the value of $q_e(\gamma_i)$ can be assumed zero for $i > i_{max}$ (i.e. $q_e(\gamma_i > \gamma_{max}) = 0$ for $i > i_{max}$), the summation for

over i in Eq.(II.48) is in fact restricted by $i \le i_{max}$. This expression together with the definition of the sequence $\{\gamma_i\}_\gamma$ in Eq.(II.46) represent the general solution of the kinetic equation for the relativistic electron distribution function in the δ-functional approximation for the kernel $C(\gamma,\gamma_1)$ in Eq.(II.37). It should be noted, however, that in this form it cannot be practically used for numerical calculations, since for the electron energies in the continuous energy loss domain, $\Delta(\gamma)/\gamma \ll 1$, the sequence of $\{\gamma_i\}_\gamma$ is too large, $i_{max} \gg 1$. In this respect it is useful to obtain the relation between the solutions given by Eqs.(II.38) and (II.48). It follows from Eqs.(II.43) and (II.44) that

$$\bar{\Delta}(\gamma) = \Delta[\gamma+\bar{\Delta}(\gamma)] \ . \qquad \text{(II.49)}$$

Using the expansion of the function $\Delta(\gamma+\bar{\Delta})$ over the power-law series of $\bar{\Delta}/\gamma \ll 1$ in the range of continuous energy losses of the electrons, the relation between the functions Δ and $\bar{\Delta}$ is readily found:

$$\bar{\Delta}(\gamma) = \frac{\Delta(\gamma)}{1-\dfrac{\partial\Delta(\gamma)}{\partial\gamma}} \equiv D(\gamma)\cdot\Delta(\gamma) \ . \qquad \text{(II.50)}$$

In compliance with the definition of the sequence $\{\gamma_i\}_\gamma$, in Eq.(II.46), we find that $\bar{\Delta}(\gamma_i)=\gamma_{i+1}-\gamma_i=\Delta(\gamma_{i+1})$. Then $\Delta(\gamma_i)D(\gamma_i)=\bar{\Delta}(\gamma_i)=\Delta(\gamma_{i+1})$. It means that in the range of continuous energy losses $\Delta(\gamma_1)\prod_{j=1}^{i} D(\gamma_i)=\Delta(\gamma_{i+1})\equiv\gamma_{i+1}-\gamma_i$ for each sequence of $\{\gamma_i\}_\gamma$. Multiplying the both sides of Eq.(II.48) by $\Delta(\gamma_1)=\gamma_1-\gamma$, the equation for $n_e(\gamma)$ can be reduced to the form:

$$n_e(\gamma) = \frac{1}{\nu_e(\gamma)\Delta(\gamma)} \left\{ \int_\gamma^{\gamma_{cr}} q_e(x)dx + \right.$$

$$\left. + \Delta_{cr}\left[q_e(\gamma_{cr}) + \sum_{i=J+1}^{i_{max}} q_e(\gamma_i) \prod_{j=J+1}^{i} D(\gamma_i)\right]\right\} \qquad \text{(II.51)}$$

Here $\Delta_{cr}\equiv\Delta(\gamma_{J-1})$, the critical energy $\gamma_{cr}\equiv\gamma_J$, and the number J is the last number i, for which the relation (II.50) is (and can be) applied. Since the electron energy loss rate can be written as

$$-\dot{\gamma} = \nu_e(\gamma)\cdot\Delta(\gamma) \ , \qquad \text{(II.52)}$$

we see that Eq.(II.51) completely coincides with the solution of the kinetic equation in continuous energy loss approximation, Eq.(II.38), if the relevant condition, $\Delta(\gamma)/\gamma \ll 1$, is valid for all γ up to γ_{max}. At the same time, Eq.(II.51) is continuously transformed into Eq.(II.48) at $\gamma=\gamma_{cr}$, if $\gamma_{cr}<\gamma_{max}$, so that at $\gamma \ge \gamma_{cr}$ the Eq.(II.48) can be used. For numerical calculations the critical energy γ_{cr} was chosen from the condition $\Delta_{cr}=(0.05\text{-}0.1)$, and in this case the characteristic number $(i_{max}-J)\le 50$, which is not too large for the numerical calculations. Note that Eq.(II.51) allows one to take easily into account (along with the Compton losses) those energy losses which contribute to $\dot{\gamma}$ at $\gamma \ll \gamma_{cr}$, in particular, the ionization ones.

5. Gamma-Radiation

In this section we obtain the gamma-ray distribution function $n_\gamma(r,\varepsilon)$ resulting at a given rate of their production $q_\gamma(r,\varepsilon)$ (in the solid angle 4π) and absorption coefficient $\varkappa_{\gamma\gamma}(r,\varepsilon)$.

Note that the radiation emitted at some site $\vec{r}_1$ in the unit volume $R_g^3 d^3 r_1$, creates at a given $\vec{r}$ the photon number density $\delta n_\gamma = q_\gamma(r_1,\varepsilon)\exp(-\Delta\tau)R_g^3 d^3 r_1/4\pi c R_g^2(\vec{r}-\vec{r}_1)^2$, where $\Delta\tau\equiv\Delta\tau(\vec{r},\vec{r}_1,\varepsilon)$ is the optical thickness with respect to gamma-ray absorption at photon-photon collisions on the way from $\vec{r}_1$ to $\vec{r}$. The

integration of δn_γ along the straight line corresponding to a given direction of gamma-ray propagation, results in the expression for the differential number density ($dn_\gamma/d\Omega$) of the gamma-rays within the solid angle $d\Omega$, which represents in fact the general solution of the relevant transport equation for gamma-rays [17]. The local number density $n_\gamma(r,\varepsilon)$ in the solid angle 4π may be obtained by integrating δn_γ over the volume $r_1 \leq r_{max} (\sim 10^8)$. For the spherically symmetric source under consideration this brings to

$$n_\gamma(r,\varepsilon) = \int_{r_0}^{r_{max}} G_\gamma(r,r_1,\varepsilon)\, q_\gamma(r_1,\varepsilon)\, dr_1 , \qquad (II.53)$$

with

$$G_\gamma(r,r_1,\varepsilon) = \frac{R_g}{2c} r_1^2 \int_{-1}^{1} \frac{d\cos\theta}{r^2+r_1^2-2rr_1\cos\theta}\, e^{-\Delta\tau(r,r_1\theta,\varepsilon)} . \qquad (II.54)$$

Here θ is the angle between the radius-vectors $\vec{r}$ and $\vec{r}_1$. In the case under consideration the optical thickness $\Delta\tau$ is due to absorption of gamma-quanta in the soft photons field $n_0(r,\varepsilon_0)$ defined by Eqs.(II.16) and (II.17). Taking into account that the absorption coefficient $\varkappa_{\gamma\gamma}=\nu_{\gamma\gamma}R_g/c$, where the collision frequency $\nu_{\gamma\gamma}$ is given by Eqs.(II.20) and (II.21), we find

$$\Delta\tau(r,r_1,\theta,\varepsilon) = \frac{R_g}{c} \int_0^{\Delta r} \nu_{\gamma\gamma}(r',\varepsilon)\, dl , \qquad (II.55)$$

where $\Delta r \equiv |\vec{r}_1-\vec{r}| = \sqrt{r^2+r_1^2-2rr_1\cos\theta}$. The integration is carried out along the straight line from $\vec{r}_1$ to $\vec{r}$, $r' \equiv |\vec{r}'|$, $l=|\vec{r}'-\vec{r}_1|$, and $\vec{r}'$ is the radius vector on this line.

In the region optically thick for gamma-rays with energy ε, i.e. corresponding to the characteristic local thickness $\tau(r,\varepsilon) \equiv \varkappa_{\gamma\gamma}(r,\varepsilon)\cdot r \gg 1$, the Eqs.(II.53) and (II.54) for $n_\gamma(r,\varepsilon)$

are significantly simplified. Indeed, in this case the integration over the entire source volume in Eq.(II.54) is efficiently reduced to integration over the small region with $\Delta r \ll r$ (due to significant increase of $\Delta\tau$ with increasing Δr), therefore Eq.(II.55) can be reduced to $\Delta\tau \simeq \nu_{\gamma\gamma}(r,\varepsilon)R_g\Delta r/c$. Taking also into account that $2\pi r_1^2 dr_1 d\cos\theta$ corresponds to the unit volume d^3r_1 which can be rewritten as $d^3r_1 = 2\pi\Delta r^2 d\Delta r d\cos\theta'$ in the spherical coordinates with the center at a given $\vec{r}$ (θ' being the angle between the vectors $\vec{r}$ and $\Delta\vec{r}\equiv\vec{r}_1-\vec{r}$), the Eq.(II.54) is reduced to

$$n_\gamma(r,\varepsilon) = \frac{q_\gamma(r,\varepsilon)}{\nu_{\gamma\gamma}(r,\varepsilon)} . \qquad (II.56)$$

This expression for $n_\gamma(r,\varepsilon)$ in optically thick region is defined only by the local values of gamma-ray absorption and emission coefficients, and is analogous to the well known expression for the photon number density in infinite homogeneous medium. The numerical calculations show that the Eq.(II.56) provides a sufficient accuracy for $n_\gamma(r,\varepsilon)$ already at $\tau(r,\varepsilon) \geq 5$.

6. Numerical Calculations of the Cascade Equations

The relations obtained above make it possible to solve numerically the problem of electron-photon cascades initiated in a spatially non-homogeneous field of soft photons due to propagation of RNs from the core of AGN (N-cascade).

Since the local number densities n_e and n_γ are determined by the sum of cascade electrons and gamma-rays of different generations, they can be represented as:

$$n_\gamma(r,\varepsilon) = n_\gamma^{(0)}(r,\varepsilon) + \sum_{i=1}^{\infty} n_\gamma^{(i)}(r,\varepsilon) , \qquad (II.57)$$

$$n_e(r,\gamma) = \sum_{i=1}^{\infty} n_e^{(i)}(r,\gamma) \ . \qquad (II.58)$$

In compliance with this, the relevant production functions of gamma-rays and electrons are:

$$q_\gamma(r,\varepsilon) = q_\gamma^{(0)}(r,\varepsilon) + \sum_{i=1}^{\infty} q_\gamma^{(i)}(r,\varepsilon) \ , \qquad (II.59)$$

$$q_e(r,\gamma) = \sum_{i=1}^{\infty} q_e^{(i)}(r,\gamma) \ . \qquad (II.60)$$

These equations correspond to the definition according to which the electrons of the i-th generation are produced due to absorption of a definite fraction of gamma-rays of the (i-1)-th generation, and further on - due to ICS of those electrons the gamma-rays of the i-th generation are produced. Note that for the sake of convenience of the numerical calculations, the initial electron production function $q_e^{(0)}$, Eq.(II.10), is related by definition to the electrons of the first generation, i.e. $q_e^{(0)}+q_e^{(1')}\to q_e^{(1)}$.

All the functions in the cascade equations are represented as one-, two-, or three-dimensional table functions with logarithmically equidistant scales of variables, i.e. $x_{k+1}/x_k=S_x=\text{const}$. In this way the large space region $10\le r\le 10^9$ and the energy range $1\le\gamma,\varepsilon\le 10^{11}$ are covered. At the first stage of calculations the kernels $S_{\gamma\gamma}(\gamma,\varepsilon)$ and $S_c(\varepsilon,\gamma)$ (i.e., the relevant table functions $S_{\gamma\gamma}(I,J)$ and $S_c(I,J)$) of the integrals in Eqs.(II.19) and (II.28) are calculated for the given background field of the soft photons $n_0(r,\varepsilon_0)$ defined by the parameters ε_c, L_{mx}/L_{Edd}, α_{rm}, and α_{mx}. Then the frequency $\nu_{\gamma\gamma}(r,\varepsilon)$ of photon-photon collisions and the kernel $G_\gamma(r,r_1,\varepsilon)$ of the integral in Eq.(II.53) are determined. For the Compton process the collision frequency $\nu_c(r,\gamma)$ and the mean electron energy loss per scattering $\Delta_e(\gamma)$ are found. From the condition

$\Delta_c(\gamma_{cr})=(0.05\text{-}0.1)$ the critical value of the electron energy γ_{cr} is determined, above which the electron distribution $n_e(r,\gamma)$ should be obtained using Eq.(II.51). Then for each discrete value γ_{cr} from the logarithmically equidistant set for the electron energy, the sequence of $\{\gamma_i\}_\gamma$ (and $\{D(\gamma_i)\}_\gamma$) satisfying Eq.(II.46) is calculated.

It should be noted that the latter procedure should be carried out only in case of a relatively weak magnetic field in the accretion plasma ($\delta_B\ll 1$), when the role of the magnetic fields is reduced mainly to isotropization of the local electron distributions not contributing significantly to the total electron energy loss rate. At the same time, in case of magnetic fields close to equipartition with the thermal electrons of accretion plasma, $\delta_B\sim 1$, the synchrotron cooling of ultrarelativistic electrons with $\gamma\ge\gamma_{cr}\sim(10^6\text{-}10^7)$ becomes greater than the Compton cooling rate (see Fig.2). Therefore, in this case the Eq.(II.38) in the continuous energy loss approximation is valid for all energies γ.

At the second stage of calculations the initial production spectra of electrons and gamma-rays, $q_e^{(0)}(r,\varepsilon)$ and $q_\gamma^{(0)}(r,\varepsilon)$, respectively, at $r_0\le r\le r_{max}=10^9$ are obtained using Eqs.(II.2-II.5) and Eqs.(II.9),(II.10). Using Eqs.(II.53) and (II.56), the number density of initial gamma-quanta $n_\gamma^{(0)}(r,\varepsilon)$ is found, and then, using Eq.(II.19), the production function $q_e^{(1)}(r,\varepsilon)$ for the cascade electrons of the first generation is obtained. Note that $q_e^{(1)}$ additively includes the initial electron production function $q_e^{(0)}$ as well. The further sequence of calculations is obvious: $q_e^{(i)}\to n_e^{(i)}\to q_\gamma^{(i+1)}\to n_\gamma^{(i+1)}\to q_e^{(i+1)}$. The spectrum of gamma-rays escaping AGN is determined from the relation $\dot{N}_\gamma(\varepsilon)=4\pi cR_g^2r_{max}^2n_\gamma(r_{max},\varepsilon)$, which implies the radial

propagation of gamma-rays in the outer regions of AGN, $r \sim r_{max}$. The direct calculations of $\dot{N}_\gamma(\varepsilon)$ using the gamma-ray production spectrum $q_\gamma(r,\varepsilon)$ and the optical thickness $\Delta\tau(r_{max},r,\theta,\varepsilon)$ testify to the validity of this assumption.

7. Results and Discussion

As is known, the basic parameter defining the characteristic features of the electron-photon cascade in a spatially homogeneous field of soft photons, i.e. of the H-cascade, is the source compactness parameter which is proportional to the ratio L_0/R, where L_0 is luminosity, and R is the characteristic size of the source (Guilbert et al. [18] defined the compactness parameter $l \equiv L_0\sigma_T/R_0 m_e c^3$; in AKV the compactness parameter was defined as $\varkappa \equiv L_0 R_g/L_{Edd} R_0 = (m_e/2\pi m_p)l$). In case of an electromagnetic cascade initiated by the RNs in a spatially non-homogeneous field of background photons, i.e. for the N-cascade under consideration, it is impossible to determine the source size analogous to R_0 of the H-cascade, since the gamma-ray spectra of different energies are formed in different scales of $r \equiv R/R_g$. At the same time, it is essential that the H-cascade is initiated due to RNs outgoing from the proton acceleration region $r \leq r_0$, and decaying at large distances from this region. Since in this case the characteristic length scale related with the neutron decay lifetime $\tau_0 \simeq 900s$, i.e. $R_n = c\tau_0 \simeq 2.7 \cdot 10^{13}$ cm is the same for all sources, then we are left with the effective "compactness" parameter for the N-cascade depending only on the integral luminosity L_{mx} of the soft photons from submillimeter up to X-ray ranges.

Indeed, for the typical power-law index $\alpha_{mx} \simeq 1$ we obtain

(using Eqs.(II.23)) that the characteristic thickness of the source at $r > r_{mx}$ with respect to absorption of initial gamma-rays with the typical energy $\varepsilon_{in}(r)$ given by Eq.(II.25) does not depend on r, and can be written as:

$$\bar{\tau}_{\gamma\gamma} \simeq (L_{mx}/1.5 \cdot 10^{43}\,\mathrm{erg \cdot s^{-1}}) \,. \qquad \text{(II.61)}$$

So, at luminosities L_{mx} less than the critical one, $L_{cr} = 1.5 \cdot 10^{43}\,\mathrm{erg \cdot s^{-1}}$, the electromagnetic N-cascade of HE and VHE gamma-rays and electrons is not developed, and the gamma-rays produced at $r \gg r_0$ easily escape AGN. At luminosities $L_{mx} > L_{cr}$ the spectrum of HE and VHE gamma-rays escaping AGN results from several cycles of the N-cascade. Since in each of these cycles some fraction of the energy is reemitted in the energy range E<100MeV, the efficiency of the cascade with respect to HE and VHE gamma-rays escaping AGN depends essentially on the characteristic number of the cascade cycles responsible for formation of the resulting gamma-ray spectra.

The spectral efficiency of the N-cascade can be defined as:

$$e(>E) \equiv \frac{L_\gamma(>E)}{\eta_n \dot{M} c^2} \,, \qquad \text{(II.62)}$$

where $L_\gamma(>E)$ is the luminosity of the source in gamma-rays with energies >E, and $\eta_n \dot{M} c^2 = \dot{W}_n$ is the total power carried by RNs out from the main power-house of AGN, $r \leq r_0$ ($\eta_n \sim 0.03$ is the efficiency of the accretion plasma rest-mass conversion to the energy of RNs, see Paper I). Note that the efficiency e(>E) cannot exceed 0.5, since according to Eqs.(II.12) and (II.13) only half of the power $\dot{W}_n$ can be transformed into the initial gamma-rays and relativistic electrons.

The partial efficiencies $e_i \equiv e_i(>E)$ which show the contribution of the i-th cascade cycle to the resulting

spectral efficiency $e\equiv e(>E)$, are presented in Table 1. The value of e_0 corresponds to the gamma-rays escaping AGN in the zeroth cycle of the cascade, i.e. this fraction of initial gamma-rays does not participate in the cascade. As it is seen from this table, the resulting efficiency e(>E) is high if the partial efficiencies of the first two cycles are high, which takes place at relatively low L_{mx}. With increasing L_{mx} ($\gg L_{cr}$) the spectral efficiency decreases, especially in the VHE range. Nevertheless, even at $L_{mx}=10^{46}$erg/s (corresponding to initial $\bar{\tau}_{\gamma\gamma}\sim 10^3$!) about 10% of the power $\dot{W}_n$ transported by RNs, can be transferred to the HE gamma-rays with E>1GeV escaping AGN. At the same time, the efficiency of the cascade in the VHE range is essentially suppressed in the sources with high L_{mx} ($\sim 10^{45}$-10^{46}erg/s).

The spectral efficiencies for $L_{mx}=10^{45}$erg/s and different values of the model parameters are presented in Table 2. It should be noted first of all that at the power-law index of accelerated protons $\alpha\simeq(2\div2.2)$ the efficiency of the N-cascade is within e(>MeV)~(25÷40)%, e(>GeV)~(5÷25)%, and e(>TeV)~(0.3÷3)%. At steeper spectra of RNs ($\alpha\sim2.5$) the efficiency is significantly below these limits, since the power contained in the VHE part of the spectrum of RNs is much less than at the hard spectra, $\alpha\sim2$.

It is seen from the results in Table 2 (at $\alpha=2.0$, $\alpha_{mx}=1.2$, but different $\dot{m}$ and δ_B), that the equipartition magnetic field of accretion plasma ($\delta_B=1$) results in a definite suppression of the cascade efficiency. The suppression factor generally does not exceed ~1.5, and it may increase up to ~2 in the VHE range (at $\dot{m}\sim3$). At the same time, at relatively weak magnetic fields (already at $\delta_B\leq0.1$) their influence on the resulting gamma-ray

spectra is negligible. It is worth noting that in this case the spectral luminosity $L_\gamma(E)$ depends linearly on the accretion rate $\dot{m}$.

The efficiencies e(>E) at different α_{mx} in Table 2 being considered, we can conclude that at least at $\alpha_{mx}\geq1$ the spectra of gamma-rays escaping AGN depends weakly on α_{mx}. At the same time, these spectra in the VHE range depend significantly on the cutoff (or flattening) of the soft photon spectrum $\varphi_0(\varepsilon_0)$ at $\varepsilon_0<\varepsilon_c$, and on the power-law exponent α_{rm} in Eq.(II.17). In Figs.3a,b the gamma-ray spectra resulting from the N-cascade are presented. Note that at gamma-ray energies $\varepsilon\equiv E/m_ec^2\geq3/\varepsilon_c$ a noticeable flattening of the spectra occurs, which is connected with the transition of the ICS process of the ultrarelativistic electrons from the Thompson scattering regime to the relativistic Klein- Nishina limit at energies $\gamma\gg\gamma_*\equiv1/\varepsilon_c$.

Another peculiarity of the gamma-ray spectra is their flattening also at lower energies, $\varepsilon\sim\varepsilon_{th}$, where $\varepsilon_{th}(\leq100)$ corresponds to the threshold energy below which the AGN region $r\leq r_{mx}\sim10^2$-10^3, responsible for formation of the background soft photon spectra, is transparent for gamma-rays with $\varepsilon<\varepsilon_{th}$. This peculiarity is due to the fact that the N-cascade is subdivided into two parts. Namely, the part of the neutron-induced cascade that is developed in the region $r\leq r_{mx}$, is related to the H-cascade type (i.e. in the homogeneous field of background photons), resulting in hard spectra of gamma-rays with moderate energies, $\varepsilon\leq\varepsilon_{th}$. The second part of the N-cascade is developed in a spatially non-homogeneous field of the background soft photons, $n_0\propto r^{-2}$ at $r>r_{mx}$, and is responsible for the formation of the gamma-ray spectra of AGN in the HE and VHE range, $\varepsilon\gg\varepsilon_{th}$. The total gamma-ray spectrum in the model under consideration

99

is determined not only by the N-cascade at $r \gg r_0$, but also by the H-cascade initiated by the gamma-rays and electrons resulting from pp collisions at $r \leq r_0$. The H-cascade is developed in the space region $r_0 \leq r \leq r_{mx}$, and it contributes to the gamma-ray spectra at energies $\varepsilon \leq \varepsilon_{th}$. Since the total power in these electrons and gamma-rays is approximately equal to the power carried out by the RNs, $\dot{W}_{\gamma e} \simeq \dot{W}_n$ (see Paper I), this contribution of the H-cascade to the resulting gamma-ray spectrum should be significant. The accurate exploration of the H-cascade spectra is done elsewhere. Here for a qualitative account of this cascade we take advantage of the results obtained by AKV, according to which the gamma-ray spectra resulting from the H-cascade, may be approximated as:

$$L_H(\varepsilon) = A\, \varepsilon^{-0.5}\, e^{-\varepsilon/\varepsilon_{th}}, \qquad (II.63)$$

where A is found from the normalization of the integral luminosity $L_H^{(tot)} = \eta' \dot{W}_{\gamma e}$, where $\eta' \sim 0.5$ is the efficiency of the H-cascade.

Note, that the gamma-rays with energies $\varepsilon \leq 10^3$ interact with the background X-ray photons $\varepsilon_0 \geq 10^{-3}$. Since the radiation spectrum of AGN in this energy range (a) is in fact formed in the region r~10-100, and (b) is described by a hard power-law spectrum with a typical exponent, $\alpha_x \sim 0.7$ [19-21] (whereas $\alpha_{mx} \geq 1$), then the real value of ε_{th} should be significantly less than it would be expected from the simplified estimation of ε_{esc} at $r = r_{mx} \sim 10^2 - 10^3$ by Eq.(II.24), i.e. the reasonable range for ε_{th} is $\varepsilon_{th} \sim (10-100)$.

Fig.4 shows the results of numerical calculations of the radiation spectra corresponding to the characteristic model parameters $\dot{m} = \dot{m}_{crm} = 2$, $\alpha_{rm} = 0$, $\varepsilon_c = 10^{-7}$, $M_8 = 1$, $\delta_B = 1$, $\Gamma_0 = 10^8$ and the threshold energy in eq.(II.63) is $\varepsilon_{th} = 10$. We can see from this figure that the spectrum $L_H(\varepsilon)$ (dotted curve) in principle can account for the spectra observed from AGN in the X-ray and soft gamma-ray bands. Moreover, the contribution of the H-cascade being taken into account, the characteristic flattening of the total gamma-ray spectrum at $\varepsilon \sim \varepsilon_{th}$ (which follows after exponential steepening of $L_H(\varepsilon)$ at $\varepsilon \geq \varepsilon_{th}$), i.e. at $E \geq (0.1\text{-}1)$GeV, becomes more pronounced.

Starting from these energies, $E \geq (0.1\text{-}1)$GeV, the gamma-ray spectrum escaping from AGN is completely due to the electromagnetic N-cascade of HE and VHE gamma-rays and electrons developed in the spatially non-homogeneous field of the background soft photons at $r \geq r_{mx}$. The spectra of HE gamma-rays can be approximated as $L(\varepsilon) \propto \varepsilon^{-\alpha_\gamma}$, with the exponent α_γ related with the power-law index α of accelerated RPs as

$$\alpha_\gamma = \alpha - 1 + \delta. \qquad (II.64)$$

Here δ is a small correction term ~0.1, depending first of all on the integral luminosity L_{mx}. In the energy range $1\text{GeV} \leq E \leq 10\text{GeV}$ the magnitude of this term is within $\delta \sim (0.0\text{-}0.03)$ for $L_{mx} = 10^{44}$erg/s, $\delta \sim (0.02\text{-}0.07)$ for $L_{mx} = 10^{45}$erg/s, and $\delta \sim (0.05\text{-}0.15)$ for $L_{mx} = 10^{46}$erg/s.

With the increase of gamma-ray energy the resulting spectrum gradually steepens. This steepening is more pronounced for the sources with higher luminosities in the submillimeter-IR band (see curves 1 and 2 in Fig.3b). Therefore, for different AGN with the same fluxes detected in the energy range, say $E \geq (1\text{-}10)$MeV, the fluxes expected in the VHE range, E>1TeV should be significantly higher for the sources with lower luminosities L_{mx}. Fig.5 presents the gamma-ray fluxes F(>E) expected from the Seyfert galaxy NGC 1275 and the quasar 3C 273 in the frames of the model proposed.

For both sources the reported HE gamma-ray fluxes are on the level $F(>100MeV)\simeq 7\cdot 10^{-7} cm^{-2} s^{-1}$ (Refs.[22] and [23], respectively; notice that the identification for NGC 1275 in [22] was presumable). The curves presented are normalized to the N-cascade gamma-ray flux $F_1(>100MeV)= 3\cdot 10^{-7} cm^{-2} s^{-1}$, assuming that the remaining flux $\Delta F=F-F_1=4\cdot 10^{-7} cm^{-2} s^{-1}$ is due to the H-cascade. The COS B observational data in the HE range $100MeV\leq E\leq 1GeV$ [23] as well as the upper limit of the WHIPPLE observatory [24] to the VHE gamma-ray flux for 3C273 are also shown. In Fig.5 the dash-dotted line is the neutrino flux $(\nu_\mu+\bar{\nu}_\mu)$ expected from these sources at $\alpha=2.0$. In the frames of the AGN model proposed, the neutrino fluxes at high energies $E\geq 1GeV$ may $\sim(2-3)$ times be greater than the gamma-ray fluxes. At the same time, this difference may be essential in the VHE range, since the neutrino spectra simply repeat the power-law spectra of the accelerated protons, whereas the gamma-ray spectra gradually steepen at higher energies.

Finally, it should be noted that the characteristic number density of e^+e^- pairs, $n_\pm(r)\sim q_e(r)/(t_a^{-1}+t_{an}^{-1})$, remains significantly less than the number density $n_T(r)$ of the accretion plasma. The numerical calculations show that the ratio $n_\pm/n_T$ is of the order 10^{-2} at $r\sim 10$, and it decreases to $n_\pm/n\sim(10^{-6}-10^{-7})$ at distances $r\sim 10^7$.

8. Conclusion

1. The main parameter defining the development of the electromagnetic N-cascade initiated by RNs is the integral luminosity L_{mx} of the source from submillimeter to X-ray bands. The critical value of L_{mx}, above which the development of the N-cascade becomes important, is $L_{cr}\simeq 1.5\cdot 10^{43}$ erg/s.

2. In contrast to the electromagnetic cascade in the spatially homogeneous field of soft photons (i.e. the H-cascade), for the neutron-induced N-cascade in the spatially non-homogeneous field of the soft photons, $n_0(r,\varepsilon_0)\propto r^{-2}$ at $r>r_{mx}$, there is no threshold energy above which the resulting gamma-ray spectra would occur. The maximal energy of the gamma-rays escaping from AGN is defined by the maximal energy of the ultrarelativistic neutrons that escape from the range $r\leq r_{mx}$ responsible for the background soft radiation.

3. With increasing L_{mx} $(>L_{cr})$ the spectral efficiency of the N-cascade, $e(>E)\equiv L_\gamma(>E)/\dot{W}_n$ (with $\dot{W}_n$ being the total power transported by the RNs from the RP acceleration region $r\leq r_0$) decreases significantly. For the power-law differential spectra of the RNs with the exponent $\alpha\simeq 2$, the cascade efficiency changes within $e(>GeV)\simeq(0.\ldots 1)$ and $e(>GeV)\simeq(6\cdot 10^{-2}-2\cdot 10^{-3})$, when the luminosity L_{mx} changes within $10^{44}-10^{46}$ erg/s, respectively. Taking into account that $\eta_n\equiv\dot{W}_n/\dot{M}c^2\sim 0.03$, we conclude that the AGN model under consideration may provide very high values of the resulting efficiency of the accretion plasma rest-mass conversion to HE and VHE gamma-rays:

$$\eta_\gamma(>E)\equiv\frac{L_\gamma(>E)}{\dot{M}c^2}=e(>E)\cdot\eta_n\ . \qquad (II.65)$$

In particular, $\eta_\gamma(>GeV)\simeq(10^{-2}-3\cdot 10^{-3})$, and $\eta_\gamma(>GeV)\simeq(2\cdot 10^{-3}-6\cdot 10^{-5})$. Thus, at accretion rates $\dot{m}\equiv\dot{M}c^2/L_{Edd}\simeq(1-3)$ the expected luminosities of AGN in HE and VHE gamma-rays are significant.

4. At lower energies, $E\leq 100MeV$, the gamma-ray spectrum is due to an electromagnetic cascade in the spatially homogeneous field of soft photons in the region $r\leq r_{mx}$. A significant contribution to the gamma-ray spectra of the source at these energies is connected with the H-cascade initiated by the

initial gamma-rays and relativistic electrons produced in the proton acceleration region $r \le r_0$. This cascade should result in formation of hard spectra from the X-ray up to soft gamma-ray bands, which steepen exponentially above some threshold energy, $E_{th} \sim (3\text{-}100)$MeV. At energies $E \gg E_{th}$ the AGN spectra are completely defined by the N-cascade, and can be described by the power-law functions $L_\gamma(E) \propto E^{-\alpha_\gamma}$ with slightly different exponents α_γ in each decade of energy E. In the HE range, E~1GeV, the exponent $\alpha_\gamma = \alpha - 1 + \delta$ with δ not exceeding ~0.1 (Eq.(II.64)). So, for $\alpha \sim 2$ a noticeable flattening of the gamma-ray spectrum of AGN at $E \ge 3E_{th}$ should be expected. In this respect the observations of the known extragalactic sources of soft gamma-radiation in the HE band 100MeV<E<10GeV, which will be possible with GAMMA-1 and EGRET (GRO) gamma-ray telescopes, will be very informative.

5. With the gamma-ray energy increasing towards the VHE range, the spectrum $L_\gamma(E)$ steepens gradually, the steepening being faster for the sources with higher luminosities L_{mx}. Therefore, the model proposed predicts that for observations in the VHE range, E≥TeV, more favourable are those AGN which: a) have relatively low integral luminosities in the submillimeter up to X-ray bands, $L_{mx} < (10^{44}\text{-}10^{45})$ erg/s; b) reveal significant fluxes of soft gamma-rays, E≥MeV; c) have broad emission line features in the IR-optical band (which is an evidence for the presence of relatively dense BL clouds at R<1kpc wherein the relativistic protons can be efficiently cooled). Note that both extragalactic sources reported so far as the VHE gamma-ray emitters, Cen A [25] and M31 [26], meet these conditions.

Amongst other known sources of soft gamma-radiation, first

of all the nearby Seyfert galaxy NGC4151 with the luminosity $L_{mx} \sim 10^{44}$erg/s should be indicated as a favourable candidate for VHE gamma-ray observations. Other candidates are the Seyfert galaxies NGC 1275 and MCG 8-11-11 having the luminosities $L_{mx} \le 10^{45}$erg/s. When considering more powerful AGN (such as N-galaxies and quasars), the VHE gamma-ray fluxes expected from them are very low, $F(\ge \text{TeV}) \le 10^{-12}\text{cm}^{-2}\text{s}^{-1}$.

6. Another peculiarity of the gamma-ray spectra of AGN in the frames of the model proposed, is their flattening at $\tilde{E} \sim \tilde{E} = 3(m_e c^2)^2/h\nu_c$, where ν_c corresponds to the low-frequency cutoff of the AGN spectrum in the IR-submillimeter band. For the typical values of $\nu_c \sim 10^{13}$Hz, the characteristic energy $\tilde{E} \sim 2 \cdot 10^{13}$eV. However, already at energies $E \ge (5\text{-}7) \cdot 10^{13}$eV the gamma-ray flux should drastically steepen due to absorption of the ultra-high-energy gamma-rays on the microwave background radiation, $T_{MBR} \simeq 2.7$K, in the intergalactic space [27,28]. Therefore, the flattening of the VHE gamma-ray spectra of AGN can be observable only for the sources with $\nu_c \ge 2 \cdot 10^{13}$ Hz.

7. At energies E~GeV the neutrino fluxes is only ~(2-3) times higher than the gamma-ray ones. This difference may become essentially greater in the VHE range due to a significant steepening of the gamma-ray spectra of the powerful sources. Therefore, for the most powerful extragalactic sources (e.g., the quasar 3C273, see Fig.5) the VHE neutrino observations by the DUMAND installation may become more effective than the gamma-ray observations of the same AGN by the existing gamma-ray Cherenkov telescopes.

Acknowledgements. I thank Dr. F.A.Aharonian for many useful discussions.

Table 1

The partial contributions $e_i(>E)$ of the i-th cycle of the N-cascade into the resulting spectral efficiency e(>E) at different luminosities L_{mx}. The model parameters are: $\alpha=2.0$, $\Gamma_0=10^8$, $\alpha_{mx}=1.2$, $\alpha_{rm}=0$, $\varepsilon_c=10^{-7}$, $r_{mx}=300$, $\delta_B=1$, $\dot{m}=1$.

L_{mx}		10^{44} erg/s		10^{45} erg/s		10^{46} erg/s	
E >		1 GeV	1 TeV	1 Gev	1 TeV	1 GeV	1 TeV
e_i/e (%)	i=0	9.50	25.0	1.37	7.86	0.11	0.91
	i=1	49.6	49.0	27.0	31.5	13.0	15.7
	i=2	31.3	21.7	43.6	41.0	41.8	44.5
	i=3	8.22	3.94	22.1	16.6	33.1	30.4
	i=4	1.19	0.38	5.17	2.76	10.3	7.51
	i=5	0.11	0.02	0.64	0.23	1.57	0.83
	i=6	-	-	0.06	0.01	0.13	0.05
$e = \sum_i e_i$		0.24	0.060	0.18	0.020	0.098	0.0022

Table 2

The spectral efficiency e(>E) of the N-cascade for different values of the model parameters α, α_{mx}, $\dot{m}$, δ_B. The other model parameters are fixed at:

$\alpha_{rm}=0$, $\varepsilon_c=10^{-7}$, $r_{mx}=300$, $L_{mx}=10^{45}$ erg/s, $M_8=1$.

α	α_{mx}	$\dot{m}$	δ_B	e(>MeV)	e(>GeV)	e(>TeV)
2.0	1.2	3	0	0.42	0.21	0.25
			1	0.27	0.13	0.010
2.0	1.2	1	0	0.42	0.21	0.25
			1	0.37	0.18	0.020
1.8	1.2	1	1	0.43	0.31	0.056
2.2	1.2	1	1	0.26	0.060	0.0034
2.2	1.0	1	1	0.27	0.062	0.0035
2.5	1.2	1	1	0.14	0.0058	0.00017

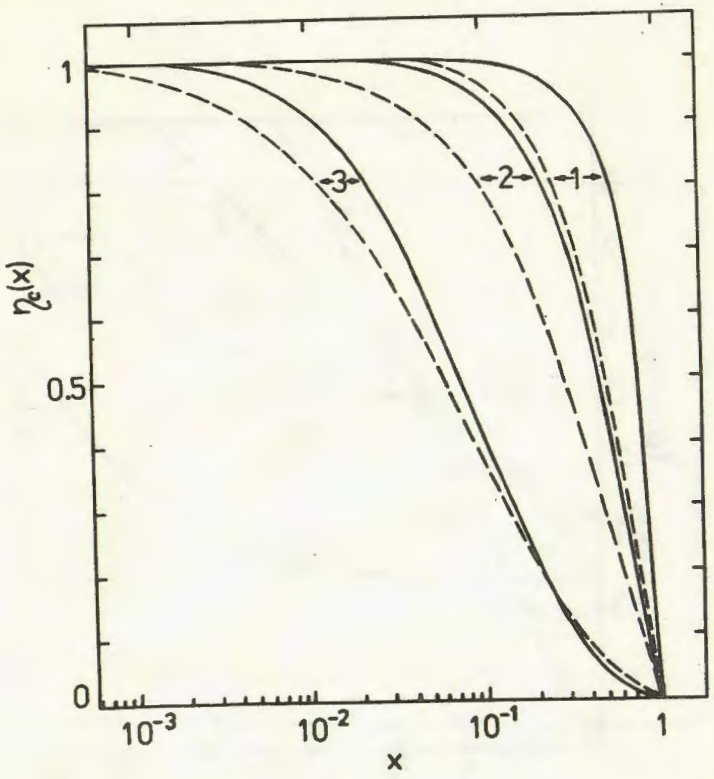

Fig.1

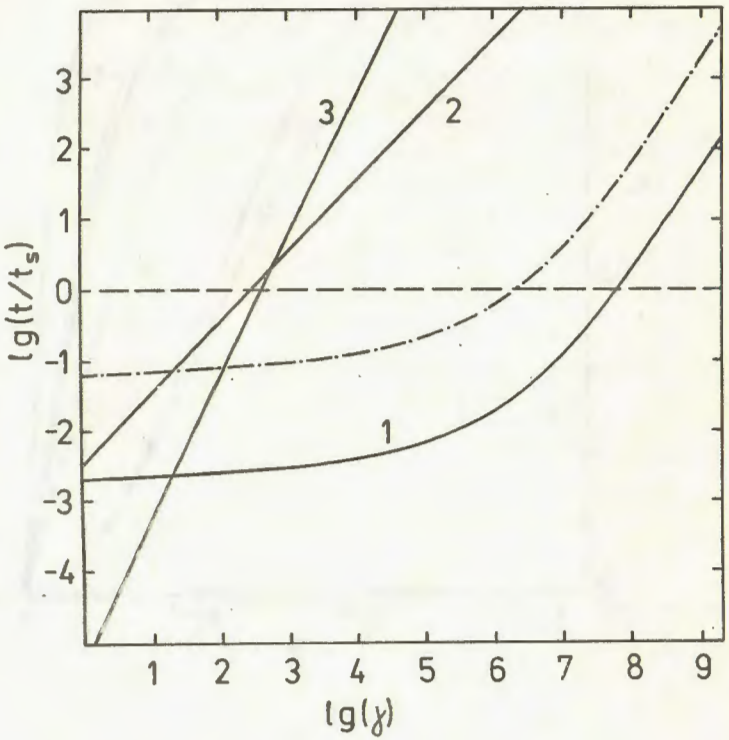
lg(t/t_s)
lg(χ)
3
2
1
3
2
1
0
-1
-2
-3
-4
1
2
3
4
5
6
7
8
9

Fig.2

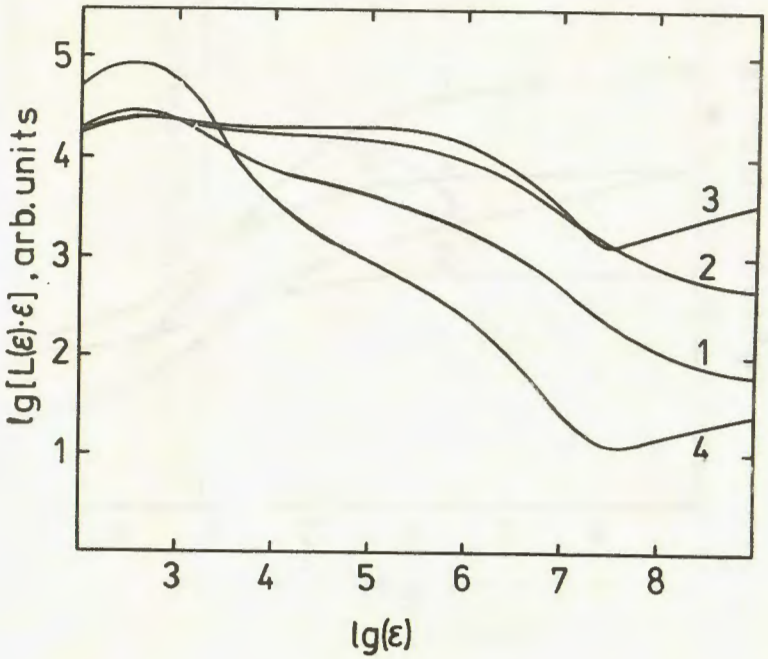
lg[L(ε)·ε], arb.units
lg(ε)
5
4
3
2
1
3
4
5
6
7
8
3
2
1
4

Fig.3a

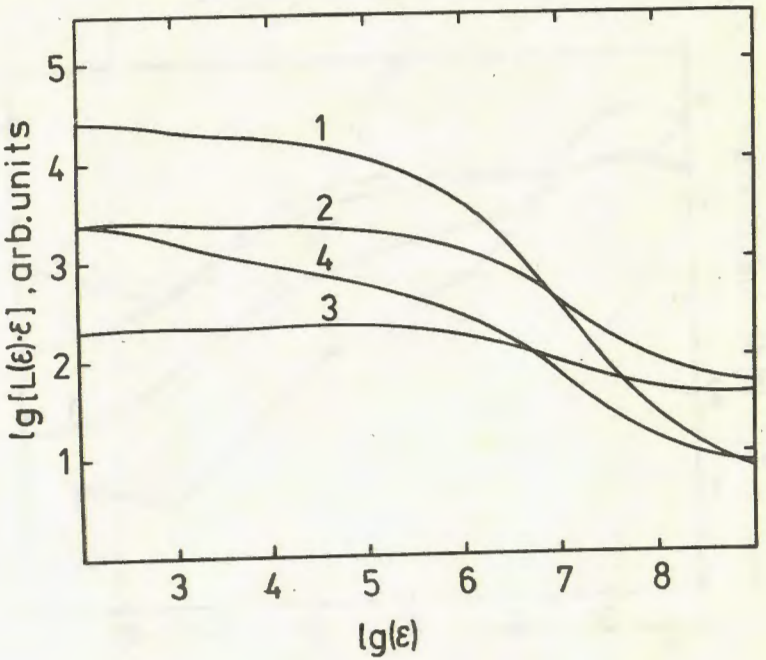
lg[L(ε)·ε], arb.units
lg(ε)
1
2
3
4
5
6
7
8

Fig.3b

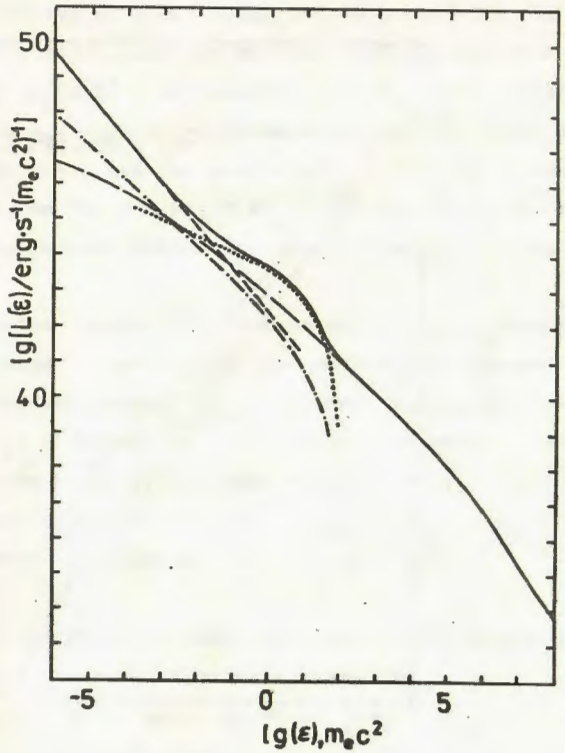
lg[L(ε)/erg·s⁻¹(mₑc²)⁻¹]
lg(ε),mₑc²
50
40
-5
0
5

Fig.4

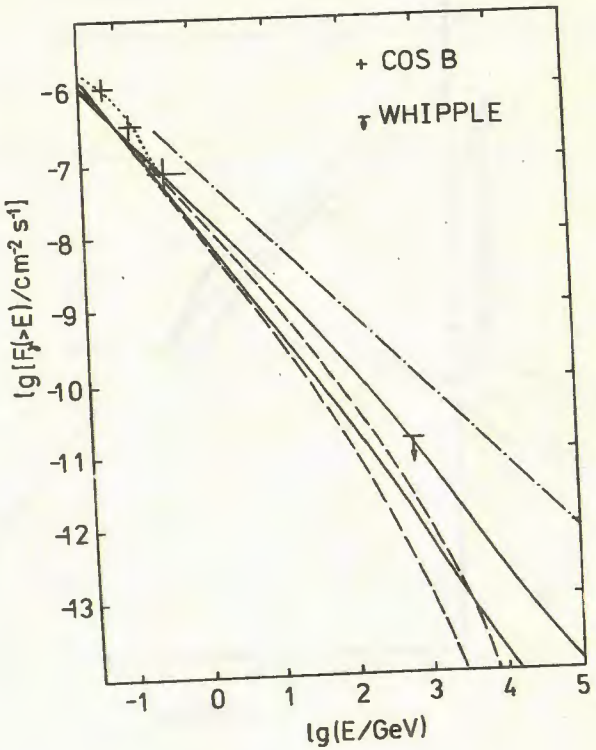

Fig.5

Figure Captions

Fig.1 The efficiency of high-energy photon production at IC/S of relativistic electrons off the soft photons with the spectrum $\varphi_0(\varepsilon_0)$, Eq. (III.17), with the power-law exponents $\alpha_{max}=1.2$, $\alpha_{min}=1$ (dashed curves), $\alpha_{max}=1.0$, $\alpha_{min}=0$ (solid curves), and for the values of $\gamma\varepsilon_c=1000$ (curve 1), $\gamma\varepsilon_c=1$ (curve 2), and $\gamma\varepsilon_c=0.01$ (curve 3); x is the ratio of the scattered photon to electron energies, $x=\varepsilon/\gamma$.

Fig.2 The electron energy loss time in different processes (1 - Compton losses, t_c; 2 - bremsstrahlung losses, t_{br}; 3 - ionization losses, t_{ion}) related to the synchrotron one, t_s, depending on the electron energy (Lorentz-factor) γ at the radius $r=10^{16}$. The model parameters are: $m=1$, $\varepsilon_c=10^{-7}$, $L_{max}=0.1L_{Eddington}$, $\delta_B=1$. The dashed curve corresponds to t_c/t_s at $r=10^{13}$.

Fig.3a,b Gamma-ray spectra resulting from the N-cascade in AGN with different sets of model parameters:

a) $M_8=1$, $\alpha_{max}=1.0$, $m=1$, $\delta_B=0$, $r_{max}=10^{13}$, $L_{max}=10^{46.5}$ erg/s, $\varepsilon_c=10^{-7}$, $\Gamma_0=10^{8}$, and: $\alpha=2.22$, $\alpha_{min}=0$ (curve 1); $\alpha=2.0$, $\alpha_{min}=0$ (curve 2); $\alpha=2.0$, $\alpha_{min}=1$ (curve 3); $\alpha=2.5$, $\alpha_{min}=1$ (curve 4).

b) $m=1$, $\alpha_{max}=1.2$, $\alpha_{min}=0$, $r_{max}=3000$, $\Gamma_0=10^{8}$, $\varepsilon_c=10^{-7}$, and: $M_8=10$, $L_{max}=10^{46}$ erg/s, $\alpha=2.0$ (curve 1); $M_8=1$, $L_{max}=10^{45}$ erg/s, $\alpha=2.0$ (curve 2); $M_8=0.1$, $L_{max}=10^{44.4}$ erg/s, $\alpha=2.0$ (curve 3); $M_8=1$, $L_{max}=10^{46.5}$ erg/s, $\alpha=2.22$ (curve 4).

Fig.4 The spectral luminosity $L(\varepsilon)$ for AGN with $M_8=1$ in a wide range of photon energies ε at characteristic parameters of the accretion plasma $\dot{m}=1$, $\delta_B=1$, of the soft radiation $L_{mx}=10^{45}$ erg/s, $r_{mx}=10^3$, $\alpha_{mx}=1.2$, $\alpha_{rm}=0$, $\varepsilon_c=10^{-7}$, and of the RNs $\Gamma_0=10^8$, $\alpha=2$,, and $\eta_n=0.03$. The short dashed, the long dashed and the dash-dotted curves are for the background soft photons, the ICS and the synchrotron radiation, respectively. The dotted curve is for the H-cascade initiated by the relativistic electrons and gamma-rays produced in the proton acceleration region $r\leq r_0$ (in the Eq.(II.63) it is supposed that $\varepsilon_{th}=10$). The total spectrum is presented by the solid line.

Fig.5 The HE and VHE gamma-ray fluxes expected from the quasar 3C273 (dashed curve) and the Seyfert galaxy NGC 1275 (solid curve) for the power-law distribution functions of accelerated RPs with exponents $\alpha=2.0$ and $\alpha=2.3$ (the upper and lower curves, respectively). The dotted curve corresponds to the total gamma-ray spectrum from 3C273, including the contribution from the H-cascade ($E_{th}=100$MeV). For 3C273 the COS B data [23] in the HE range as well as the recent upper limit of the WHIPPLE observatory [24] to the VHE gamma-ray flux are given. The dashed line corresponds to the neutrino fluxes expected from these sources at $\alpha=2.0$.

References

1. Atoyan A.M. //Preprint YERPHI-1268(55)-90, Yerevan 1990.
2. Atoyan A.M., Nahapetian A. //Astron. Astrophys., 1989, v.219, p.53.
3. Aharonian F.A., Vardanian V.V., Kirillov-Ugryumov V.G. //Astrophysics, 1984, v.20, p.118 (Astrofizika, 1984, v.20, p.223).
4. Aharonian F.A., Vardanian V.V. //Astrophys. Sp. Sci., 1985, v.115, p.31.
5. Aharonian F.A., Kirillov-Ugryumov V.G., Vardanian V.V. //Astrophys. Sp. Sci., v.115, p.201; (AKV).
6. Svenssen R. //M.N.R.A.S., 1987, v.227, p.403.
7. Zdziarski A.A. //Ap. J., 1988, v.335, p.786.
8. Murzin V.S., Sarycheva L.I. //Physics of Hadronic Processes, Energoizdat, Moscow, 1986.
9. Aharaonian F.A., Atoyan A.M., Nahapetian A.//Astrophysics, 1983, v.19, p.187 (Astrofizika, 1983, v.19, p.323).
10. Herterich K. //Nature, 1974, v.250, p.311.
11. Zdziarski A.A. //Ap.J., 1989, v.342, p.1108.
12. Ginzburg V.L., Syrovatskii S.E. //Sov. Phys. JETP, 1964, v.46, p.1865.
13. Blumenthal G.R., Gould R.J. //Rev.Mod.Phys., 1970, v.42, p.237.
14. Pacholczyk A.G. //Radio Astrophysics, Freeman, San Francisco, 1970.
15. Akhiezer A.I., Berestetskii V.B. //Quantum Electrodynamics, Nauka, Moscow, 1969.
16. Aharonian F.A., Atoyan A.M. //Sov. Astron. AJ Lett., 1981, v.7, p.714.

17. Atoyan A.M., Nahapetian A.G.//Astrofizika, 1990 (in press).
18. Guilbert P.W., Fabian A.C., Rees M.J. //M.N.R.A.S., 1983, v.205, p.593.
19. Mushotsky R.F., Marshall F.E., Holt S.S., Serlemitsos P.J. //Ap. J., 1980, v.235, p.377.
20. Rothshield R.E. et al. //Ap. J., 1983, v.268, p.68.
21. Worall D.M., Marshall F.E. //Ap.J., 1984, v.276, p.434.
22. Strong A.W., Bignami G.F. //Ap.J., 1983, v.274, p.549.
23. Bignami G.F. et al, //Astron. Astrophys., 1981, v.93, p.71.
24. Vacanti G. et al. //Proc. 21st ICRC, Adelaida, 1990, v.2, p.329.
25. Grindlay et al. //Ap.J.Lett., 1975, v.197, p.L9.
26. Dowthwaite J.C. et al. //Astron. Astrophys., 1984, v.136, p.L14.
27. Aharonian F.A. Atoyan A.M. //Sov. Phys. JETP, 1985, v.89, p.337.
28. Protheroe R.J. //M.N.R.A.S., 1986, v.221, p.769.

The manuscript was received June 6, 1990

А.М. АТОЯН
РЕЛЯТИВИСТКИЕ НЕЙТРОНЫ В ЯДРАХ АКТИВНЫХ ГАЛАКТИК
2. ГАММА-ИЗЛУЧЕНИЕ ВЫСОКИХ И ОЧЕНЬ ВЫСОКИХ ЭНЕРГИЙ
(на английском языке, перевод Г.А. Папяна)
Редактор Л.П.Мукаян
Технический редактор А.С.Абрамян

Подписано в печать 25/IX-90 ВФ-01461 Формат 60×84×16
Офсетная печать. Уч.изд.л. 2 Тираж 299 экз.Ц.30 к.
Зак.тип. 257 Индекс 3649

Отпечатано в Ереванском физическом институте
Ереван-36, ул. Братьев Алиханян 2.

The address for requests:
Information Department
Yerevan Physics Institute
Alikhanian Brothers 2,
Yrevan, 375036
Armenia, USSR